

Scaling of fracture strength in ZnO: Effects of pore/grain-size interaction and porosity

Chunsheng Lu^{a,b,c,*}, Robert Danzer^a, Franz Dieter Fischer^b

^a *Institut für Struktur- und Funktionskeramik, Montanuniversität Leoben, A-8700 Leoben, Austria*

^b *Institut für Mechanik, Montanuniversität Leoben, A-8700 Leoben, Austria*

^c *School of Aerospace, Mechanical and Mechatronic Engineering, Centre for Advanced Materials Technology (CAMT), The University of Sydney, Sydney, NSW 2006, Australia*

Received 10 July 2003; received in revised form 24 November 2003; accepted 7 December 2003

Available online 10 May 2004

Abstract

Recent experiments on the fracture strength of zinc oxide (ZnO) ceramics showed that the size of specimens has almost no influence on their mean strength although strength data of a set of nominally identical specimens are still found to scatter. It is suspected that the complex nature of defect–microstructure interaction and the high density of porosity in ZnO ceramics are possible reasons for this insensitivity to strength scaling. In the paper, numerical results obtained by finite element analysis show that the fracture strength of ZnO is more influenced by the pore/grain-size interaction than only by the size of a pore or its shape. As a consequence, the pore/grain-size interaction will increase the fracture probability of small pores and lead to a homogenisation of critical flaw sizes. Furthermore, the high degree of porosity, especially the heterogeneous distribution and clustering of pores, could favour further homogenisation of critical crack sizes. This implies that the fracture strength of ZnO is insensitive to the size of specimens as corroborated by experiments. Finally a simple statistical explanation is given.

© 2004 Elsevier Ltd. All rights reserved.

Keywords: Fracture strength; Grain size; Porosity; ZnO; Finite element method

1. Introduction

Ceramics have been widely applied in engineering due to their excellent resistance to heat, corrosion, and wear. But, ceramics also are very sensitive to flaws and have a disposition to brittle failure. Their fracture strength, i.e., the maximum stress they can withstand, varies unpredictably from component to component even if a set of nominally identical specimens are tested under the same conditions. Generally speaking, the strength of brittle materials decreases as the size of specimens increases, and this so-called size effect can be well described by Weibull statistical fracture theory.^{1–7} Recent experiments on the fracture strength of electroceramics, however, have shown that it is not always so. The strength data of zinc oxide (ZnO), applied for varistors, are still found to scatter, but the size of specimens has

no evident influence on their mean strength.^{8–10} The latter is obviously in conflict with Weibull statistical theory.

Extensive fractographic investigations of ceramics have shown that the failure usually originates from pre-existing defects (such as inclusions, microcracks and pores), which may arise from their intrinsic microstructures or imperfect processing.^{11–13} In most cases, fracture strength of ceramics, similar to other brittle materials, is controlled by the properties of critical flaws or microstructures (such as size, shape, orientation, etc.). As an example, grain size has a clear effect on fracture strength of ceramics. For a coarse grained material fracture strength shows a strong increase with decreasing grain size. Conversely, for the fine grained materials, fracture strength increases only slightly or remains constant with decreasing grain size.^{14–16}

As is well known, electroceramics, such as ZnO and barium titanate (BaTiO₃), are mainly designed and optimised with respect to their electrical rather than mechanical properties as in the case for structural ceramics like silicon nitride (Si₃N₄), silicon carbide (SiC), etc. and thus they usually contain a high degree of porosity which might act

* Corresponding author. Tel.: +61-2-9351-2348; fax: +61-2-9351-7060.

E-mail address: chunsheng.lu@aeomech.usyd.edu.au (C. Lu).

as the origin of fracture. Although mechanical properties including elastic modulus, strength, and toughness usually decrease with increasing porosity in brittle materials, it is suspected that the complex nature of defect–microstructure interaction and the high density of porosity are possible reasons for the insensitivity to strength scaling discovered in ZnO ceramics.^{8–10} In order to verify this hypothesis, and more generally, to understand the scaling behaviour of the strength of electroceramics containing high densities of flaws, the effects of pore/grain-size coupling and porosity on the fracture strength in ZnO need to be investigated.

In this paper, based on experimental results and fractographic observations, several finite element models are proposed to explore the intrinsic mechanism or causes of the observed behaviour in ZnO ceramics. The basic principle of Weibull strength distribution and experimental results are briefly introduced in the following section. Then the description of finite element models and main numerical results are given in Sections 3 and 4. Finally a simple statistical explanation is suggested in Section 5, and a short summary is attached in Section 6.

2. Strength distribution and size effect

Fracture strength of brittle materials is strongly related to the details of defects, such as their sizes, orientation, distributions, etc. It is often supposed that a small volume element in a brittle material is like a link of a chain with many links. If any link breaks, then the whole material will fail. Based on this weakest link principle and an empirical power law function, a statistical distribution function of wide applicability, i.e., the well known Weibull distribution, was proposed.^{5–7} Here the cumulative failure probability of a brittle material subjected to an applied stress σ can be represented as:

$$P(\sigma, V) = 1 - \exp \left[-\frac{V}{V_0} \left(\frac{\sigma}{\sigma_0} \right)^m \right], \quad (1)$$

where V is the volume of a specimen, V_0 is the reference volume, σ_0 is the characteristic strength, and m is the Weibull modulus, which is a measure of the scatter of strength data.

If two specimens with different sizes have the same probability of failure, from Eq. (1) it is easy to obtain

$$V_1 \sigma_1^m = V_2 \sigma_2^m. \quad (2)$$

Obviously the size effect is a direct consequence of the Weibull distribution. In other words, the larger the size of a specimen, the higher the probability of finding a critical defect and the smaller the strength of the corresponding sample.^{1–3} For an inhomogeneous uniaxial stress state, such as a miniature 4-point flexural strength test¹⁷ the above relationship can be represented as

$$V_{\text{eff},1} \sigma_{\text{max},1}^m = V_{\text{eff},2} \sigma_{\text{max},2}^m, \quad (3)$$

where V_{eff} is the effective volume subjected to the maximum stress σ_{max} . This provides us with another experimental procedure to test and verify the Weibull statistical distribution.

Recently, fracture strengths of three ceramic materials, i.e., Si_3N_4 , SiC and ZnO, were tested, more details on the experiments have been reported in other papers.^{8,9} As illustrated in Fig. 1, for Si_3N_4 and SiC, the mean strength decreases with the increase of the effective volume of a specimen. In the case of ZnO, however, the mean strength of specimens remains almost constant with the increase of their effective volumes, that is to say, there is no clear size effect as would be expected from the Weibull distribution, see solid arrow lines in Fig. 1.

The Weibull distribution has been found to successfully describe a large number of fracture data from brittle materials. This does not mean, however, that the Weibull distribution is always in preference to other distributions, such as the normal, log-normal distributions, etc. As the amount of samples used in experiments is limited, it is often very difficult to clearly distinguish between the Weibull and other distributions in some real cases. In order to highlight the difference between two possibly favourite distributions, we introduced a simple quantitative procedure, i.e., the so-called Akaike information criterion (AIC), which is defined as $\text{AIC} = -2 \ln \hat{L} + 2k$, where $\ln \hat{L}$ is the maximum log-likelihood for a given distribution and k is the number of parameters to be fitted in the distribution.^{9,18} Then it was applied to the fit of strength data of three ceramic materials mentioned above. The results showed that, for Si_3N_4 and SiC, the Weibull distribution fits the data better than the normal distribution, but in the case of ZnO, the result is just the opposite, and the normal distribution may be a preferred choice.⁹

Strictly speaking, the hypotheses formulated to get the Weibull distribution are not always correct or necessary in real applications. Based on as few assumptions as possible (mainly the weakest link concept and no interaction between defects), a general strength distribution can be derived as:^{19–21}

$$P(\sigma, V) = 1 - \exp[- \langle N_c(\sigma, V) \rangle], \quad (4)$$

where $\langle N_c(\sigma, V) \rangle$ is the expectation value of critical defects in a specimen of size V . Note here, that the weakest link argument does not yield any specific form for $\langle N_c(\sigma, V) \rangle$. In general, the flaw density strongly decreases as the flaw size a increases, and then the frequency distribution $n(a)$ can be approximated by a simple inverse power law

$$n(a) = n_0 \left(\frac{a}{a_0} \right)^{-r}, \quad (5)$$

where n_0 , a_0 , and r are material parameters. In addition, a crack-like defect is often found in brittle materials, and, based on the Griffith fracture criterion, the relationship between a critical flaw size a_c and fracture strength σ_f can be

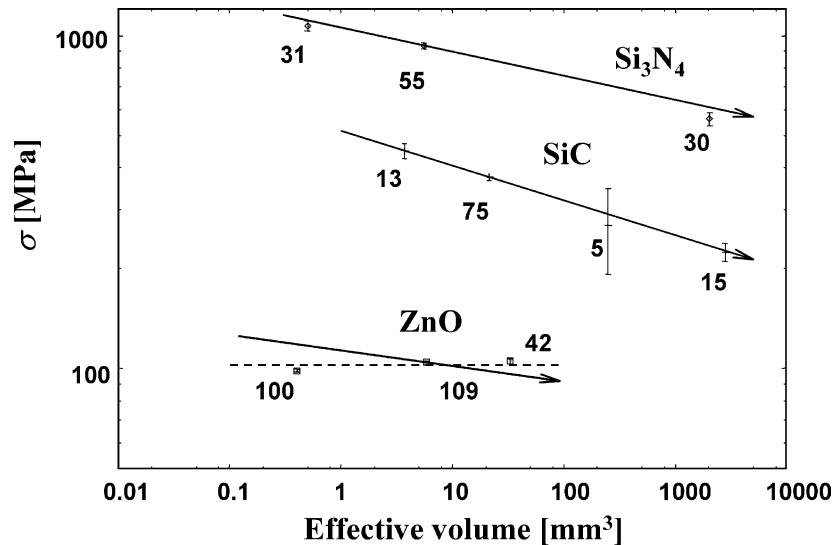


Fig. 1. Experimental results for three ceramics regarding the dependence of mean strengths on effective volumes. Numerals are the number of experiments, and error bars refer to the 95% confidence band (the higher the number of tests, the smaller the scatter of data). Solid arrow lines, with a slope of $-1/m$, indicate the size effect extrapolated by the Weibull distribution. Here the Weibull moduli m determined by the sample with the single size and the largest specimens (55 for Si_3N_4 , 75 for SiC and 109 for ZnO) are 13.9, 9.6, and 20.9 for Si_3N_4 , SiC and ZnO, respectively. The dashed line indicates the arithmetic mean strength $\sigma_f = 102.37$ MPa of the sample with the largest specimens.

represented as

$$a_c = \frac{1}{\pi} \left(\frac{K_c}{Y\sigma_f} \right)^2, \quad (6)$$

where K_c is the critical stress intensity factor and Y is a dimensionless geometrical factor.^{1–3} Inserting Eqs. (5) and (6) into Eq. (4), we can easily obtain the Weibull distribution function, as indicated by Eq. (1), and the Weibull modulus which characterises the size distribution of flaws, $m = 2(r - 1)$. So it becomes obvious from these observations that the Weibull distribution is only a special case of this general strength distribution function. This can provide us with some hints for the understanding of experimental discoveries, such as the effects of inhomogeneous or multi-modal flaw distribution, the R -curve behaviour, high porosity, etc. However, more comprehensive investigations on the relationship between fracture strength and microstructures should be conducted. Although almost all established methods of designing with ceramic materials are based on the Weibull statistics, in cases like the ZnO ceramics mentioned above, designing on this theory could lead to an overestimation or underestimation of the tolerable design stress, as shown in Fig. 1.

3. Description of the models

Recent experiments on electroceramic components, such as high power varistors and positive temperature coefficient (PTC) switching components, showed that failure starts at internal flaws which could be traced back to green bodies or powder agglomerates.^{11–13} Due to the trend to increase power densities in electrical devices, the mechanical loads

imposed on these components increase, and problems with insufficient mechanical strength get more and more severe. It is surprising, however, that relatively few investigations exist about the mechanical failure of electroceramics.¹³

As exemplified in Fig. 2, the real configuration of flaws in ZnO ceramics is very complex. In a first approximation, the intrusions formed by impingement of neighbouring grains can be described by a Saturn ring-like crack around a pore. Based on fractographic evidence, a mechanical model for brittle fracture must take into account the interaction of two different defect populations: intrinsic defects on the microstructural level such as grain boundaries which are regarded as nucleation sites for microcracks, and processing defects such as pores or inclusions that act as stress concentrators.^{14–16}

In the ZnO ceramics discussed above, a typical flaw is represented by a pore with cusps or sharp grooves, as can be seen in Fig. 2a and is modelled in Fig. 3a. Here there are three characteristic length scales: the pore radius R , the grain radius r , and the notch depth c . If the groove angle $\theta = 0$, the notch depth c can be determined by a simple relationship, $c = \sqrt{R(R + 2r)} - R$, that is to say, the independent parameters shrink to two, and the sharp groove is similar to a crack with curved faces. According to fractographic investigations on ZnO ceramics, the mean radius R of critical pores is in the range of 25–100 μm , and the radius r of grains is in the range of 2–10 μm .^{11–13} The mechanical properties of ZnO are: the elastic modulus $E = 100$ GPa and Poisson's ratio $\nu = 0.36$.²² In addition, it is worth noting that the degree of porosity in ZnO is as high as 5 vol.%. Due to the heterogeneous distribution of defects, often clusters exist formed by a group of pores, as can be seen in Fig. 2b and is illustrated in Fig. 3b, and even clustering of sub-clusters occurs.

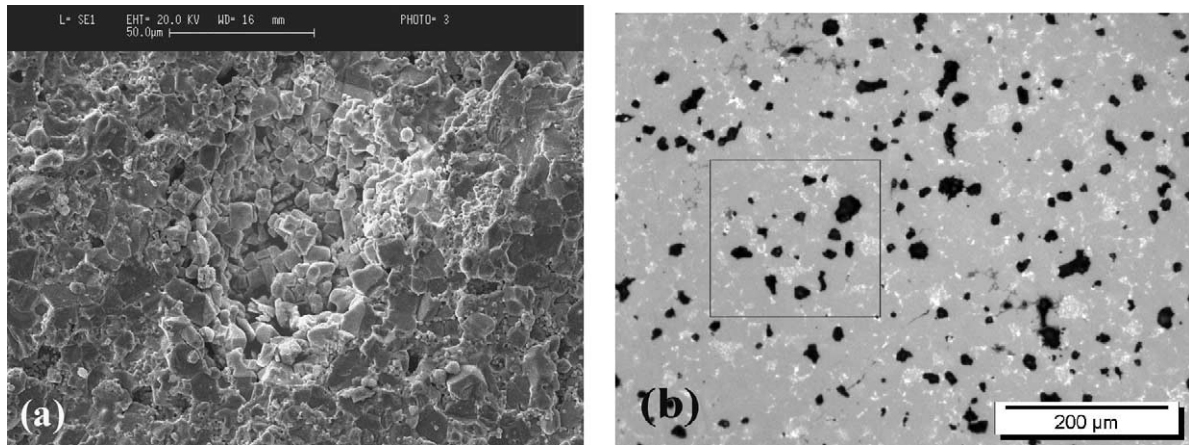


Fig. 2. A typical fracture origin (a) and a cluster of pores (b) in ZnO ceramics.

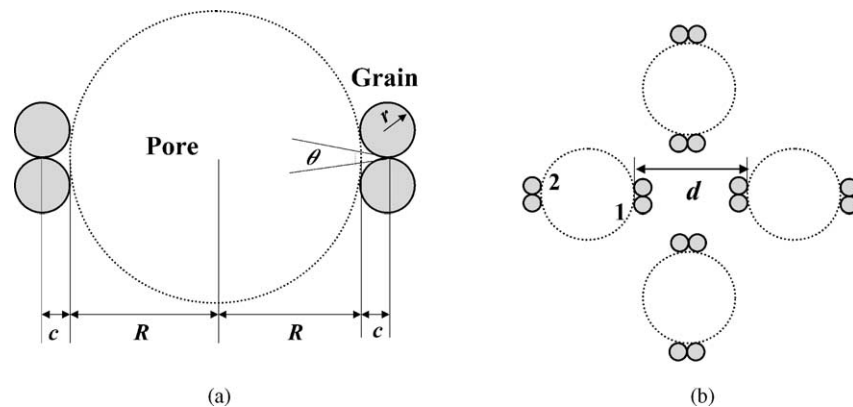


Fig. 3. Sketch of two-dimensional models of defects in ZnO ceramics. (a) A single pore with cusps or sharp grooves formed by neighbouring grains, and (b) a typical cluster formed by several pores due to heterogeneous distribution of defects. d is the internal distance of the cluster, the numbers 1 and 2 indicate the inner and outer cracks, respectively.

Thus, the interaction (the stress shielding or intensification) between pores or clusters may also play an important role in determining the fracture strength of ZnO ceramics.

4. Finite element analysis

Several approaches exist for the analytical and numerical investigations of materials with a certain flaw distribution. Maybe the most direct method is to study a multicroack system based on the theory of elasticity and conformal mapping or numerical methods.^{23,24} A second approach can be described by a lattice model for the simplest discretisation of a material with flaws.^{25,26} A third approach is closely related to the concept of continuum damage mechanics.²⁷ Here the numerical tools such as the finite element method may be applied more easily for realistic defect configurations to be investigated. In the following analysis, the stress fields and stress intensity factors for a pore with sharp grooves or its cluster, as illustrated in Fig. 3, are evaluated using the finite element code ABAQUS/Standard V.5.8 (Hibbitt, Karlsson and Sorensen Inc., 1998, <http://www.hks.com>);

meshing was mainly carried out with the preprocessor code PATRAN V.9.0 (MacNeal-Schwendler Corp., 1998, <http://www.mscsoftware.com>).

It is worth noting that the two-dimensional model used here attempts to simplify the numerical calculations and provide a rough approximation for the understanding of the general tendency of the effects of pore/grain interaction on strength, but more sophisticated three-dimensional analyses, as in some recent works,^{14–16} are needed in order to get an exact equation for the effects of pore/grain-size interaction and porosity.

4.1. Stress singularity of a sharp groove

For the sake of simplicity, let the radii (R and r) of a pore and grains surrounding the pore be constants, as shown in Fig. 3a. Different notch angles θ can be obtained via the change of the depth c to a groove tip. The cases for every 10° interval of θ were chosen, and the stress field in the vicinity of a sharp groove was calculated. The results show that, as we expected, the stress singularity takes the form $\sigma \propto r^{-\alpha}$, where the singularity order α is closely related to the angle θ

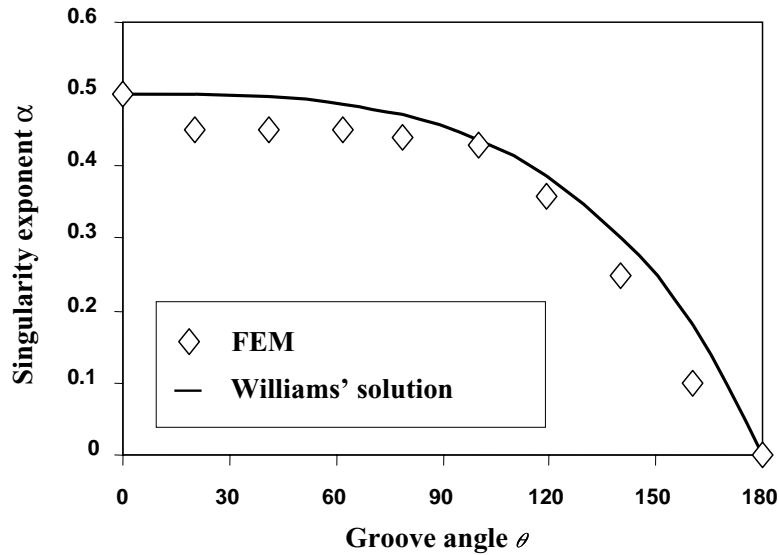


Fig. 4. The stress singularity exponent α in the vicinity of a sharp groove vs. its angle θ . For comparison Williams' analytical result for a sharp notch is also plotted (solid line).

of a groove, and changes from 0.5 ($\theta = 0^\circ$) to 0 ($\theta = 180^\circ$) (see Fig. 4). The detailed structure of the groove-tip stress field differs from that of a common crack. Specifically, this singularity still exists even under compressive stress since groove surfaces do not touch.

The problem of the stresses in the notch edge vicinity was solved by Williams.²⁸ The relationship between the singularity order α and the notch angle θ can be represented by $\sin [(1 - \alpha)(2\pi - \theta)] - (1 - \alpha) \sin \theta = 0$. (7)

It is obvious to see that the stress singularity of a sharp groove is weaker than that of a sharp notch, as shown in Fig. 4. The difference to Williams' analytical result reflects the influence of the groove shape. Here it is of interest to note that the singularity order $\alpha = 0.5$ if $\theta = 0$, and the groove reduces to a crack-like sharp notch. In fact such a sharp groove is often developed in order to keep the surface energy to a minimum, and it is the case we will discuss in the following.

4.2. Effect of pore/grain-size interaction on fracture

Recent development of ABAQUS allows for studies of the stress intensity factors in a multicroack system in which a domain integral technique is used to calculate the contour integral J . This method can provide high accuracy with relatively coarse meshing. It is worth noting that, as illustrated in Fig. 3, the crack (i.e., sharp groove) faces are curved, and a positive stress intensity factor also exists in the case of global compressive loading. The normals to the crack faces that lie within the domains used for the contour integrals must be specified in the calculation in order to keep the J -integral to be path independent. At the same time, finite strain analysis is used in order to model the possible large displacement field around the groove tip under compressive

loading. Once J values are known, the stress intensity factors can be obtained by

$$K = \sqrt{\frac{JE}{1 - \nu^2}}. \tag{8}$$

Three kinds of pores ($R = 25, 50, \text{ and } 100 \mu\text{m}$) with sharp grooves, formed by various grain sizes were calculated. The stress intensity factors of a pore with sharp grooves can be written as

$$K = F \left(\frac{r}{R} \right) \sigma \sqrt{\pi c}, \tag{9}$$

where F is a correction factor.^{29,30} For a shallow groove ($r \ll R$), the crack tip is embedded within the local stress concentration of a pore and $F \approx 1.12 \times 3 = 3.36$. As one might expect, F drops quickly when r increases because the crack runs out of the high stress concentration region (see Fig. 5).

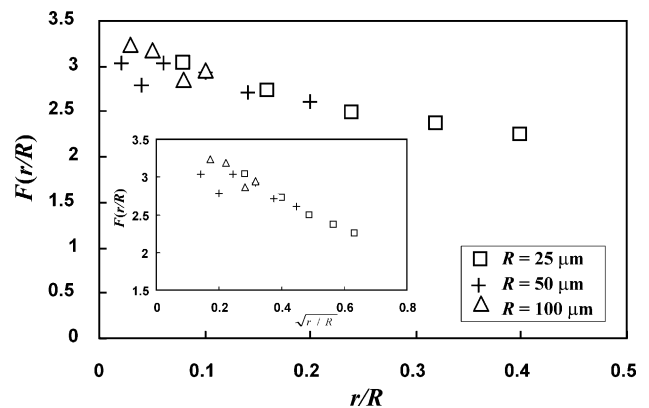


Fig. 5. The geometric correction factor $F(r/R)$ vs. the ratio of grain and pore sizes r/R . The inset shows the relationship between $F(r/R)$ and the square root of r/R .

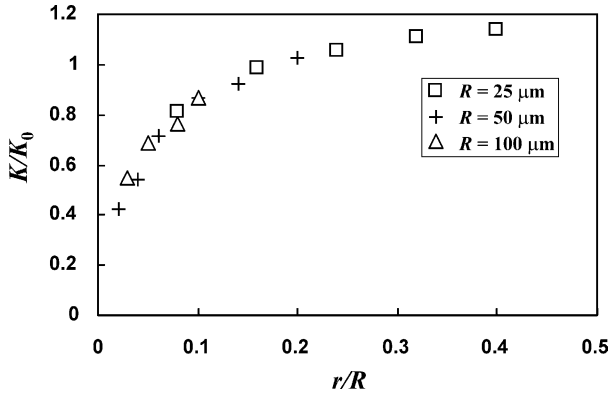


Fig. 6. The normalised stress intensity factor vs. the ratio of grain and pore sizes. Here three kinds of pores with radius $R = 25, 50,$ and $100 \mu\text{m}$ were calculated. The depth of a sharp groove c can be determined by the simple geometrical relationship, $c/R = \sqrt{1 + 2r/R} - 1$. Here $K_0 = \sigma\sqrt{\pi(R + c)}$. For more details of the model, see Fig. 3a.

For the cases studied here, the pore should be considered as a part of the crack. Fig. 6 shows the variation of the normalised stress intensity factor, K/K_0 , versus the ratio of grain and pore sizes, r/R . Here we define the stress intensity factor for a crack with the length $(R + c)$ as a reference, i.e., $K_0 = \sigma\sqrt{\pi(R + c)}$, where σ is the nominated stress used in the calculation. It is easy to see that the normalised stress intensity factor K/K_0 is closely related to the ratio of grain and pore sizes. For smaller pores and constant grain size, the normalised stress intensity factor is greater than that for big ones. In other words, the size distribution of critical flaws tends to be more homogeneous. Here

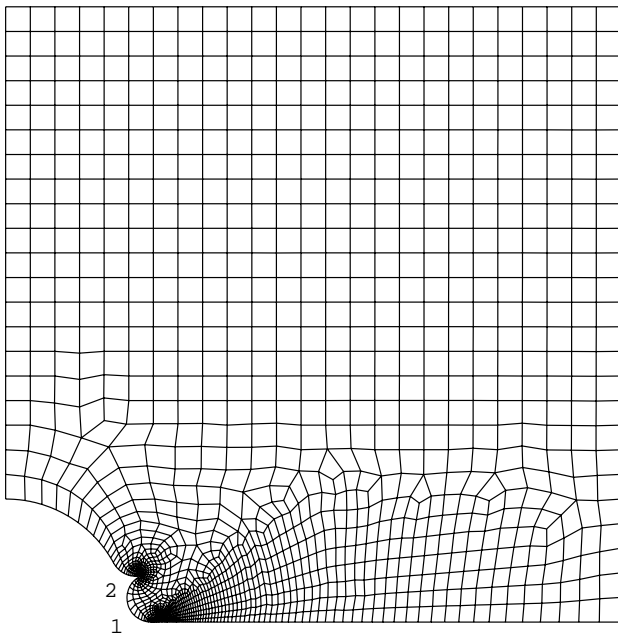


Fig. 7. A more realistic finite element model of defects in ZnO ceramics. Here $R = 50 \mu\text{m}$ and $r = 10 \mu\text{m}$, and 8-node plane strain elements are used in the analysis. Due to the geometrical symmetry, the quadrant of the model is considered.

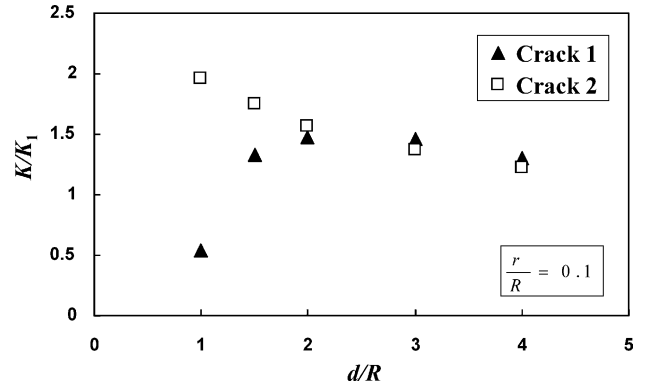


Fig. 8. The normalised stress intensity factor vs. the ratio of cluster and pore sizes for a single cluster of pores. Here K_1 indicates the stress intensity factor of a single pore, and $r/R = 0.1$. For more details of the model, see Fig. 3b.

a caution should be given that numerical errors increase as the ratio r/R becomes bigger, but the tendency is not influenced.

The real configuration of a pore in ZnO ceramics is much more complex than that we supposed in this simple model. One may argue that at least two or more grooves should be used to simulate the irregular concave surface shape formed by grains surrounding a pore. Further numerical analysis for a more realistic model was carried out, in which three sharp grooves were introduced (Fig. 7). Note here, that the crack 2 lies in a mixed-mode loading, and the J -integral does not distinguish between modes of loading. However, this difficulty can be overcome by using the crack face displacements. The result showed that the stress intensity factor at the middle groove tip (crack 1 in Fig. 7) decreases by 12% compared to that of the single groove as indicated above due to the shielding influence of its neighbouring grooves. Compared to the influence of the ratio of grain and pore sizes discussed above, it is less important and was omitted for simplicity.

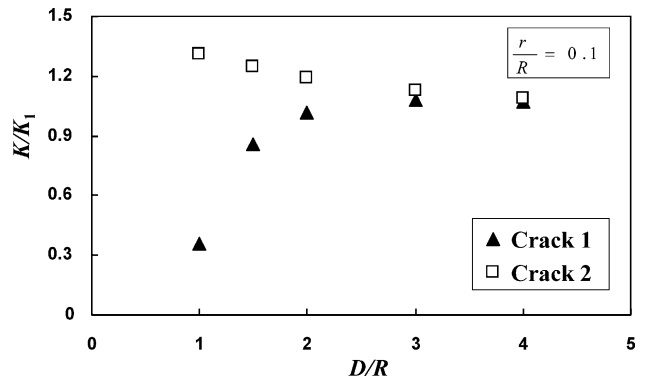


Fig. 9. The normalised stress intensity factor vs. the ratio of cluster and pore sizes for clustering with a periodic distribution. Here D indicates the distance between two clusters, K_1 is the stress intensity factor of a single pore, and $r/R = 0.1$. For more details of the model, see Fig. 3b.

4.3. Effect of porosity on fracture

In general many ceramics have some degree of porosity. It is intuitively evident that elastic moduli and strength will

decrease as porosity increases. This is an open and difficult problem although considerable research has been done. As is well known, the interaction between defects is sensitive to the details of their geometrical arrangement. Especially the

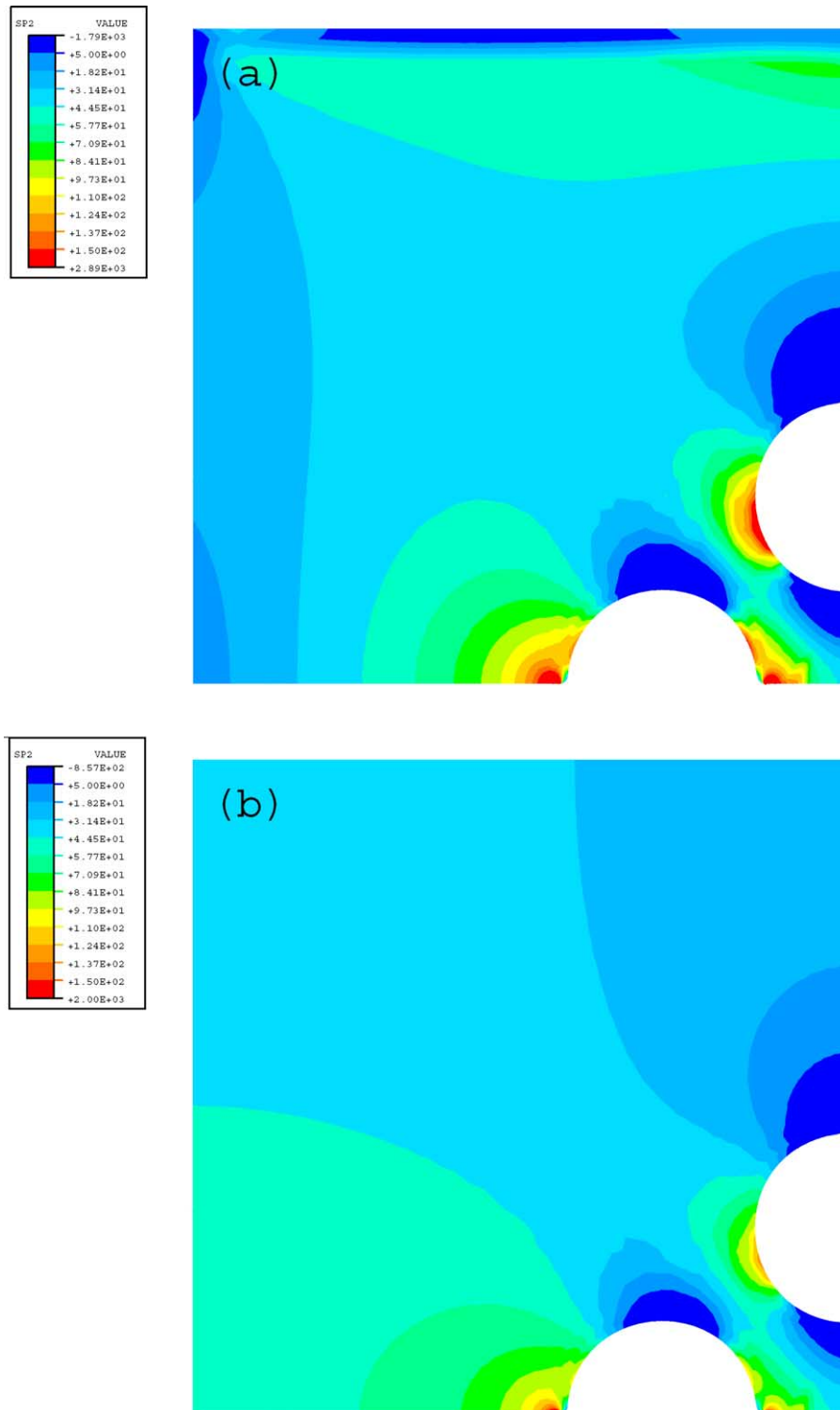


Fig. 10. The maximum principal stress patterns due to the interaction of pores in a single cluster (a) and a clustering with a periodic distribution (b), where red colour represents the highest stress and the dark blue represents the lowest stress. Here $r/R = 0.1$, $d/R = 2$, and $D/R = 2$. The tensile load $\sigma = 100$ MPa is applied along the vertical direction, and the periodic boundary conditions are introduced in (b).

mechanical properties such as fracture strength discussed here are closely related to local rather than average properties; consequently it is not easy, and even impossible to establish a deterministic relationship.^{23,31,32} Next, in order to qualitatively understand the possible influence of the high degree of porosity on the fracture strength of ZnO ceramics, two typical cases are studied: one being a single cluster as illustrated in Fig. 3b and the other a periodic distribution of the single cluster.

As shown in Fig. 8, shielding for the inner crack, i.e., the crack 1 in Fig. 3b, will be effective if the distance between pores approaches a certain threshold. Due to heterogeneous distribution of microstructures and defects, clustering of defects is often found in specimens. The main reason can be a multi-modal powder size distribution. Here the clustering behaviour is modelled by a periodic array of clusters with distance D , which is defined as the distance between the centres of two clusters. The shielding effect discussed above is more evident as shown in Fig. 9. The stress intensity factor of the inner crack decreases when the ratio d/R is about less than two, which corresponds approximately to 5 vol.% for pores uniformly distributed in the specimen. The normalised stress intensity factors of both inner and outer cracks decrease, as comparing the stress distribution for the two cases (Fig. 10). This means that clustering will further increase the homogeneities of critical flaw sizes, at least for this special defect configuration in ZnO ceramics. We should also notice that the results obtained here are merely instructive and qualitative but, at the same time, the approximation of two-dimensional model will lead to an overestimation of shielding.

5. Discussion and a simple statistical explanation

The absence of the size effect discovered from experiments on the fracture strength of ZnO ceramics manifests a deviation from the Weibull distribution. Another distribution such as normal or log-normal distribution might be used in the analysis of strength data, which has been corroborated by further statistical analysis. As discussed above, the grain size has a clear effect on the fracture strength of ZnO ceramics. It is usually found that grain size distributions measured are approximately log-normally distributed.³³

Contrary to Si_3N_4 and SiC ceramics where crack-like flaws are sparsely distributed, flaws in ZnO ceramics, i.e., pores with sharp grooves, are determined by many independent and random factors such as size, location, even the degree of porosity, etc. Thus we can expect that strength data yield the Weibull distribution in Si_3N_4 and SiC ceramics, but it is not so in ZnO ceramics. The probability of a flaw becoming critical in ZnO ceramics may be described $p = \prod p_i$, where p_i denotes the probability of i th influential driver. So taking logarithms of both sides we have $\log p = \sum \log p_i$. Since p_i are independent random variables, the

central limit theorem is applicable, and $\log p$ has a normal distribution just as we expected.

As a consequence of the interaction of pore/grain size and a high porosity in ZnO ceramics, a group of pores as well as their cluster could affect the final fracture compared to only the largest defect as the Weibull weakest link model postulates. Here we attempt to give a simple statistical explanation. Let us suppose that the number of defects in a given specimen is N , and the failure probability of a defect is p . For the sake of simplicity, the interaction between pores is neglected. The failure probability of n defects can thus be written as $P_N(n) = \{N!/n!(N-n)!\} p^n (1-p)^{N-n}$. As is well known,³⁴ there are two special cases for this binomial distribution in the limit of large N . If p is not too small (this seems to be corresponding to the case of ZnO), the binomial distribution is approaching the normal distribution. By contrast, if $p \ll 1$, we have the Poisson distribution $P_N(n) = a^n \exp(-a)/n!$, where $a = Np$. Next, let $n = 0$ one can easily obtain $P_N(0) = \exp(-Np)$ and then the weakest link model can be described in the form $F = 1 - P_N(0) = 1 - \exp(-Np)$. Compared with Eq. (4), obviously the Weibull distribution is only a special case, and thus it is not surprising that no size effect was discovered in ZnO ceramics (see Fig. 1).

Finally, it is worth noting that the results obtained here are based on a two-dimensional model. The three-dimensional configuration of defects in ZnO ceramics could be described by a spherical pore with some kinds of sharp cracks, such as a circumferential crack, a semicircular crack, and a circular crack.^{14–16} The numerical analysis of the three-dimensional model is much more complex since we need to consider the special configuration of defects and their arrangement, but is worthy of investigation in the future. At the same time, the behaviour could also be explained by other possible reasons such as the presence of the R -curve characteristics as commonly observed in ceramics, which often reduces the strength variability.^{35,36}

6. Concluding remarks

Based on both experiments of fracture strength and numerical analysis of the effects of pore/grain-size interaction and porosity on fracture strength in ZnO ceramics, the following conclusions can be drawn:

- The Weibull distribution could be widely used in the analysis of strength data and size effect. Recent experiments on the fracture strength of electroceramics, however, have shown that it is not always so. The strength distribution may be the normal or other distributions rather than the Weibull distribution due to the influence of many independent and random factors.
- The stress singularity of a sharp groove formed by grains around a pore is closely related to its angle.

- The fracture strength in ZnO ceramics is more influenced by the ratio of pore and grain sizes or pore/grain-size interaction than only by the size of critical pores. As a consequence the pore/grain-size interaction increases the fracture probability of small pores and decreases the fracture probability of large pores. This fact yields a homogenisation of the critical flaw sizes.
- The high degree of porosity, especially the heterogeneous distribution and clustering of pores, could favour further homogenisation of critical crack sizes in ZnO ceramics.

Acknowledgements

This work was supported by the Lise Meitner Programme of the Austrian Science Fund (FWF) under project numbers M587 and M662. We are grateful to Prof. F.G. Rammerstorfer and Dr. H.J. Böhm for many valuable discussions.

References

1. Lawn, B. R., *Fracture of Brittle Solids (2nd ed.)*. Cambridge University Press, Cambridge, 1993.
2. Wachtman, J. B., *Mechanical Properties of Ceramics*. John Wiley & Sons, Inc., New York, 1996.
3. Bažant, Z. P. and Planas, J., *Fracture and Size Effect in Concrete and Other Quasibrittle Materials*. CRC Press, Boca Raton, 1998.
4. Rice, R. W., *Mechanical Properties of Ceramics and Composites*. Marcel Dekker, Inc., New York, 2000.
5. Weibull, W., A statistical distribution function of wide applicability. *J. Appl. Mech.* 1951, **18**, 293–297.
6. Freudenthal, A. M., Statistical approach to brittle fracture. In *Fracture, Vol II*, ed. H. Liebowitz. Academic Press, New York, 1968, pp. 591–619.
7. Jayatilaka, A., de, S. and Trustrum, K., Statistical approach to brittle failure. *J. Mater. Sci.* 1977, **12**, 1426–1430.
8. Danzer, R. and Lube, T., Fracture statistics of brittle materials: it does not always have to be Weibull statistics. In *Ceramic Materials and Components for Engines*, ed. K. Niihara. Japan Fine Ceramics Association, Tokyo, 1998, pp. 683–688.
9. Lu, C., Danzer, R. and Fischer, F. D., Fracture statistics of brittle materials: Weibull or normal distribution. *Phys. Rev. E* 2002, **65**, 067102.
10. Lu, C., Danzer, R. and Fischer, F. D., Effects of pore/grain-size interaction and porosity on the fracture of electroceramics. In *Fracture Mechanics of Ceramics, Vol 14/15*, ed. R. C. Bradt et al. Plenum Press, New York, in press.
11. Danzer, R., Mechanical failure of advanced ceramics: the value of fractography. *Key Eng. Mater.* 2002, **223**, 1–18.
12. Supancic, P., Fracture and fractography of electroceramics. *Key Eng. Mater.* 2002, **223**, 69–78.
13. Danzer, R. and Supancic, P., Mechanical failure and mechanical design of electroceramic components. In *Ceramic Engineering and Science Proceedings, Vol 24, No.4*, Cocoa Beach, FL, 2003, pp. 21–26.
14. Zimmermann, A., Hoffman, M., Flinn, B. D., Bordia, R. K., Chuang, T.-J., Fuller, Jr. E.R. et al., Fracture of alumina with controlled pores. *J. Am. Ceram. Soc.* 1998, **81**, 2449–2457.
15. Zimmermann, A. and Rödel, J., Generalized Orowan–Petch plot for brittle fracture. *J. Am. Ceram. Soc.* 1998, **81**, 2527–2532.
16. Zimmermann, A. and Rödel, J., Fracture statistics based on pore/grain-size interaction. *J. Am. Ceram. Soc.* 1999, **82**, 2279–2281.
17. Lube, T., Manner, M. and Danzer, R., The miniaturisation of the 4-point-bend test. *Fatigue Fract. Eng. Mater. Struct.* 1997, **20**, 1605–1616.
18. Lu, C., Danzer, R. and Fischer, F. D., Fracture statistics of brittle materials: how to choose a better distribution function. In *Fracture Mechanics Beyond 2000, Vol 2*, ed. A. Neimitz et al. EMAS Publishing, Warley, 2002, pp. 395–400.
19. Danzer, R., A general strength distribution function for brittle materials. *J. Eur. Ceram. Soc.* 1992, **10**, 461–472.
20. Danzer, R. and Lube, T., New fracture statistics for brittle materials. In *Fracture Mechanics of Ceramics, Vol 11*, ed. R. C. Bradt et al. Plenum Press, New York, 1996, pp. 425–439.
21. Danzer, R., Lube, T. and Supancic, P., Monte Carlo simulations of strength distributions of brittle materials—type of distribution, specimen and sample size. *Z. Metallkd.* 2001, **92**, 773–783.
22. Shackelford, J. F., Alexander, W., Park, J. S., *Materials Science and Engineering Handbook*. CRC Press, Boca Raton, 1994.
23. Kachanov, M., Elastic solids with many cracks and related problems. *Adv. Appl. Mech.* 1994, **30**, 259–445.
24. Kachanov, M., Solids with cracks and non-spherical pores: proper parameters of defect density and effective elastic properties. *Int. J. Fract.* 1999, **97**, 1–32.
25. Meakin, P., Models for material failure and deformation. *Science* 1991, **252**, 226–234.
26. Lu, C., Vere-Jones, D. and Takayasu, H., Avalanche behaviour and statistical properties in a microcrack coalescence process. *Phys. Rev. Lett.* 1999, **82**, 347–350.
27. Krajcinovic, D., *Damage Mechanics*. North-Holland, Amsterdam, 1996.
28. Williams, M. L., Stress singularities resulting from various boundary conditions in angular corners of plates in extension. *J. Appl. Mech.* 1952, **19**, 526–528.
29. Tada, H., Paris, P. and Irwin, G., *The Stress Analysis Handbook*. Del Research Cooperation, St. Louis, MO, 1985.
30. Hertzberg, R. W., *Deformation and Fracture Mechanics of Engineering Materials*. John Wiley & Sons, Inc., New York, 1996.
31. Rice, R. W. and Lewis, D., Limitation and challenges in applying fracture mechanics to ceramics. In *Fracture Mechanics of Ceramics, Vol 5*, ed. R. C. Bradt, A. G. Evans, D. P. H. Hasselman and F. F. Lange. Plenum Press, New York, 1983, pp. 659–676.
32. Shields, E. B., Fracture prediction of hole patterns with multiple cracks using the finite element method. *Int. J. Fatigue* 2001, **23**, 13–20.
33. Bennett, E., Lay, L., Morrell, R. and Roebuck, B., *Microstructural Measurements on Ceramics and Hardmetals, Measurement Good Practice Guide No. 21*. National Physical Laboratory, London, 1999.
34. Reichl, L. E., *A Modern Course in Statistical Physics*. University of Texas Press, TX, 1980.
35. Damani, R. J., Schuster, Ch. and Danzer, R., Polished notch modification of SENB-S fracture toughness testing. *J. Eur. Ceram. Soc.* 1997, **17**, 1685–1689.
36. Mai, Y.-W., Cohesive zone and crack-resistance (R) curve of cementitious materials and their fibre-reinforced composites. *Eng. Fract. Mech.* 2002, **69**, 219–234.